Metal–Organic Frameworks

International Edition: DOI: 10.1002/anie.202000299
German Edition: DOI: 10.1002/ange.202000299

Protein-Structure-Directed Metal–Organic Zeolite-like Networks as Biomacromolecule Carriers

*Huanrong Wang[+], Lin Han[+], Dong Zheng, Mingfang Yang, Yassin H. Andaloussi, Peng Cheng, Zhenjie Zhang, Shengqian Ma, Michael J. Zaworotko, Yifan Feng, and Yao Chen**

Abstract: *Fabrication of zeolite-like metal–organic frameworks (ZMOFs) for advanced applications, such as enzyme immobilization, is of great interest but is a great synthetic challenge. Herein, we have developed a new strategy using proteins as structure-directed agents to direct the formation of new ZMOFs that can act as versatile platforms for the in situ encapsulation of proteins under ambient conditions. Notably, protein incorporation directs the formation of a ZMOF with a sodalite (**sod**) topology instead of a non-porous diamondoid (**dia**) topology under analogous synthetic conditions. Histidines in proteins play a crucial role in the observed templating effect. Modulating histidine content thereby influenced the resultant MOF product (from **dia** to **dia** + **sod** mixture and, ultimately, to **sod** MOF). Moreover, the resulting ZMOF-incorporated proteins preserved their activity even after exposure to high temperatures and organic solvents, demonstrating their potential for biocatalysis and biopharmaceutical applications.*

In the past decades, zeolite-like metal–organic frameworks (ZMOFs, also referred to metal–organic zeolites, MOZs) have emerged as a metal–organic analogues of inorganic zeolites and are an important subclass of MOFs because they can integrate the merits of both MOFs and zeolites,[1–3] such as, high porosity thanks to cage-like cavities,[2] designable pore window/shape,[4] customizable functionality,[5] and exceptional stability.[6] ZMOFs have become an active field of MOF chemistry as they offer potential utility for applications as diverse as gas storage/separation,[7] drug delivery,[8] sensing,[9] enzyme immobilization,[10–13] and so on.[14–16] Theoretically, the number of ZMOFs is vast, as reflected by the high number of hypothetical zeolite topologies and the modular nature of MOFs databases.[17,18] However, ZMOFs are still rare among the 75 600 MOF entries in version 5.38 of the Cambridge Structural Database. This is largely because the synthesis of ZMOFs requires control of network topology and functionality. This is difficult because the assembly of tetrahedral building blocks (namely, the fundamental building blocks of zeolitic networks such as ZMOFs) tends to result in the default **dia** topology, which is not a zeolitic topology.

Template-directed synthesis has proved to be a powerful strategy to obtain new ZMOFs that are otherwise inaccessible.[19] For example, the presence of different templates, such as 1,2-diaminocyclohexane, imidazole, 1,3,4,6,7,8-hexahydro-2*H*-pyrimido[1,2-a]pyrimidine (HPP), afforded **mer**, **sod**, and **rho** Z-MOF topologies, respectively.[2,3] If the template(s) remains after MOF synthesis, additional functionalities, such as chirality,[20] catalysis,[21] and fluorescence,[22] can be transferred from templates to such "template@MOF" materials (@ = encapsulated by). Until now, template molecules have typically comprised small inorganic,[23] organic[24] or organic–inorganic species[25] and the use of proteins as templating agents is yet to be reported. In polymer chemistry, proteins have been applied as removable templates to fabricate molecularly imprinted polymers (MIPs), which can be used for protein recognition.[26] These results inspired us to explore if proteins, especially bioactive enzymes, can indeed be used as templates to form new ZMOFs which can inherit the function of proteins (for example, catalysis,[27,28] recognition, and sensing[29]). In this study, we demonstrate the use of proteins as templates to direct the formation of a new ZMOF platform with zeolitic sodalite or **sod** topology (named hereafter **ZPF-1**, ZPF = zeolitic pyrimidine framework, Scheme 1). In contrast, the same experiment conducted in the absence of a protein template afforded the default **dia** network. **ZPF-1** can thereby serve as a versatile platform for the in situ encapsulation of proteins with high loading capacity because the protein remains in the material after synthesis. We also investigated the mechanism of templating to study the role of histidines on proteins in directing the target ZMOF structure. The discovery of the templating effect of proteins and a more developed understanding of the mechanism should provide guidance for the design and synthesis of a broad range of functional porous materials that incorporate biomacromolecules.

Many MOFs are designed according to the "node and linker" approach and elaborated using "reticular chemistry".[30] The key design concept in generating protein-encapsulating ZMOFs (for example, **ZIF-8** and **ZIF-90**)[10–12] is the

[*] H. Wang,[+] D. Zheng, Prof. Z. Zhang, Y. Feng, Prof. Y. Chen
State Key Laboratory of Medicinal Chemical biology,
College of Pharmacy, Nankai University, Tianjin 300071 (China)
E-mail: chenyao@nankai.edu.cn
L. Han,[+] M. Yang, Prof. P. Cheng, Prof. Z. Zhang
College of Chemistry, Nankai University, Tianjin 300071 (China)
Prof. S. Ma
Department of Chemistry, University of South Florida
4202 E. Fowler Avenue, Tampa, FL 33620 (USA)
Y. H. Andaloussi, Prof. M. J. Zaworotko
Department of Chemical Sciences, Bernal Institute,
University of Limerick, Limerick V94 T9PX (Republic of Ireland)
Prof. Y. Chen
National Institute for Advanced Materials, Nankai University
Tianjin 300071 (China)
[+] These authors contributed equally to this work.
Supporting information and the ORCID identification number(s) for the author(s) of this article can be found under:
https://doi.org/10.1002/anie.202000299.

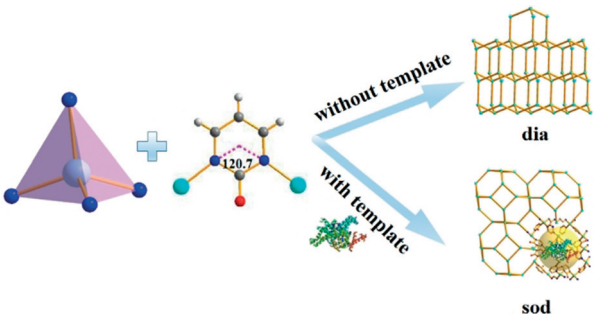

Scheme 1. Illustration of the template effect of proteins to direct the formation of new zeolitic frameworks (**sod** topology) encapsulating proteins, instead of forming the default **dia** topology. Color code: carbon (gray), hydrogen (white), nitrogen (blue), metal (cyan), and oxygen (red).

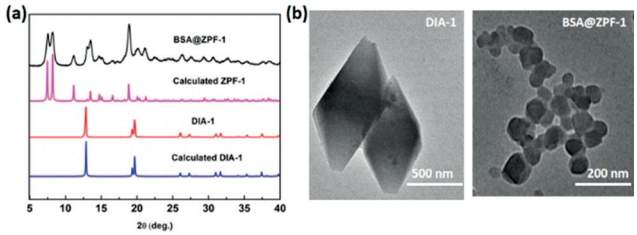

Figure 1. a) PXRD patterns of the **BSA@ZPF-1** and **DIA-1** compared with calculated patterns; b) TEM images of **DIA-1** (left), **BSA@ZPF-1** (right).

tetrahedral geometry of the metal atoms (for example, Zn^{2+}) and a suitable subtended linker angle (for example, 142.4° for 2-R-imidazole, R = methyl or aldehyde). Pyrimidine derivatives are a basic building block of genetic material and possess structural similarity with the imidazole derivatives that generate **ZIF-8** and **ZIF-90**. However, the use of pyrimidin-2-ol and zinc ions to generate ZMOFs has not been achieved by traditional synthesis methods, which afford the previously reported nonporous MOF (named herein **DIA-1**) with diamond morphology and **dia** topology (Supporting Information, Figure S1). Herein, inspired from the protein-template effect in the formation of MIPs, we show that use of proteins as templates to modulate the reactions of pyrimidin-2-ol and zinc cations is feasible, thereby preparing ZMOFs that encapsulate proteins.

Bovine serum albumin (BSA) was selected as a model protein in this study on the basis of its low cost and high solubility. Presence of BSA during synthesis resulted in a new crystalline phase (named herein **ZPF-1**) in aqueous solution at room temperature. Fourier transform infrared spectroscopy (FT-IR) (Supporting Information, Figure S2a) confirmed that successful encapsulation of BSA into **ZPF-1** had occurred, indicated by the existence of characteristic peaks of BSA. Fluorescein isothiocyanate (FITC)-labeled BSA was also encapsulated by **ZPF-1** and scanned by CLSM (confocal laser scanning microscopy, Supporting Information, Figure S2b) to further verify that successful encapsulation of BSA had indeed occurred. Calculations based on the Bradford method revealed that the loading of BSA is as high as 0.2365 $g\,g^{-1}$. Powder X-ray diffraction (PXRD) and transmission electron microscopy (TEM) studies were conducted to further verify and investigate the template effect of BSA (Figure 1 and Supporting Information, Figure S3). Peak broadening observed in the PXRD pattern of **BSA@ZPF-1** revealed the presence of nanometer-scale crystals, which was verified as such using TEM. As shown in Figure 1b, **BSA@ZPF-1** formed particles approximately 80 nm in size and polyhedral morphology, whereas **DIA-1** formed particles with dimensions on the order of 600 nm and prismatic morphology. Gas sorption data revealed the **BSA@ZPF-1** exhibited a hierarchal structure with both ultra-micro pores originated from the structure nature of **ZPF-1** and macro pores due to particle packing or defects (Supporting Information, Figure S4). Furthermore, the obtained MOF product was shown to be affected by the concentration of BSA. A mixture of **BSA@ZPF-1** and **DIA-1** was obtained when reducing the amount of BSA (less than 0.05 $mg\,mL^{-1}$, Supporting Information, Figure S5). These results show that BSA indeed exhibits a template effect that enables the formation of **ZPF-1.**

On the basis of the templating effect of BSA, we studied if other proteins could also serve as templates. The template effect was indeed broadly observed for proteins, such as GOX (glucose oxidase), Mb (myoglobin), insulin, CAT (catalase), ACP (acid phosphatase), and G-IgG (goat anti-BSA IgG polyclonal antibody), all of which templated the formation of **ZPF-1** (Supporting Information, Table S1), as verified by PXRD (Supporting Information, Figure S6) and TEM (Supporting Information, Figure S7). FT-IR spectroscopy results confirmed that proteins were successfully encapsulated into **ZPF-1** (Supporting Information, Figure S8). This broad performance across a range of proteins prompted us to investigate the mechanism behind the templating effect. As the basic building blocks of proteins, amino acids were first tested. After screening all 20 natural amino acids, we found that only histidine templated the formation of **ZPF-1** (Supporting Information, Figure S9) at room temperature from aqueous solution. Single crystal X-ray diffraction (SCXRD) data revealed that each zinc atom is four-coordinated in a tetrahedral geometry connected to bridging pyrimidin-2-ol ligands to generate a three-dimensional (3D) network with **sod** topology that resembles the structure of **ZIF-8** and **ZIF-90**. Compared with the regular sod cages of **ZIF-8** and **ZIF-90**, with inner cage diameters of approximately 7 Å, **ZPF-1** possessed a smaller **sod** cage of approximately 6 Å diameter (Figure 2). PXRD analysis revealed that samples of **protein@ZPF-1** matched the calculated pattern of **ZPF-1** (Figure 1a and Supporting Information, Figure S6).

We subsequently discovered that the amount of added histidine can affect the outcome. PXRD (Supporting Information, Figure S10) tests revealed a mixture of **DIA-1** and **ZPF-1** when reducing the concentration of histidine. This effect is consistent with that observed for BSA. In order to exclude other possible factors that may affect the templating process (for example, anions and metal–ligand ratio), we varied the zinc salts (for example, $ZnCl_2$, $Zn(OAc)_2$, $ZnSO_4$, and $Zn(ClO_4)_2$) and the ratios of reactants with no influence on the topology of the final product (Supporting Information,

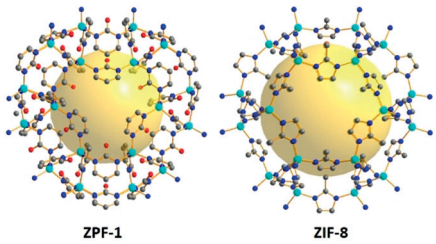

Figure 2. Structural diagram of **ZPF-1** vs. **ZIF-8**. Color code: carbon (gray), hydrogen (white), nitrogen (blue), and oxygen (red).

Figures S11 and S12). Control reactions were performed whereby macromolecules without histidines were added, such as organic polymers (polyethylene glycol (PEG), polyvinyl alcohol (PVA), polyvinylpyrrolidone K30 (PVP)), antibiotics (streptomycin and chloramphenicol), and inorganic particles (SiO_2 and Fe_3O_4), all of which failed to generate the **ZPF-1** product (Supporting Information, Figure S13). These results reveal that the template effect of proteins originates from presence of histidine.

We attribute these observations to histidine being an α-amino acid with an imidazole functional group. Indeed, histidine has already been incorporated into the **sod** network of **ZIF-8** as a co-ligand due to its similar coordination geometry to 2-methyl imidazole.[31,32] We found that 2-methyl imidazole can also template the formation of **ZPF-1**, once again indicative of the key role of imidazole moieties in the templating process (Supporting Information, Figure S14). Thus, it is reasonable to assert that the imidazole moieties in histidine can form structural precursors of the **sod** network in the initial reaction stage and thereafter be substituted by excess pyrimidin-2-ol in the following step to generate the observed **sod** network (Scheme 2). If the above assertion is correct, the amount of histidine in proteins (Supporting Information, Table S1) is likely to influence their templating effect. Thus, we treated BSA with diethyl pyrocarbonate (DEPC), a histidine-specific alkylating reagent (Figure 3a). As the alkylation reaction of DEPC progressed, the UV absorbance of BSA at 227 nm increased (Figure 3b). The absorbance at 227 nm had no obvious upward trend from 60 min to 120 min after DEPC treatment, indicating that the alkylation reaction had reached equilibrium at 60 min (Figure 3a,b). When DEPC-modified BSA was used as an additive in the reaction of pyrimidin-2-ol and zinc ions, **DIA-1** was produced with the absence of **ZPF-1** (Supporting

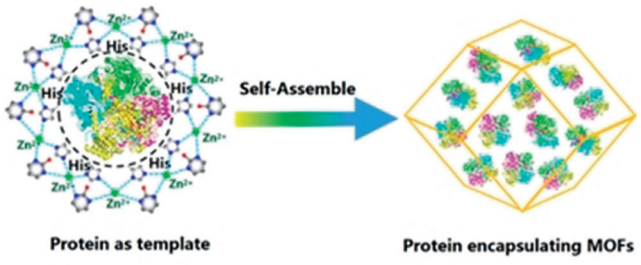

Scheme 2. A proposed process for the histidine-induced templating effect in the generation of ZMOFs for protein encapsulation.

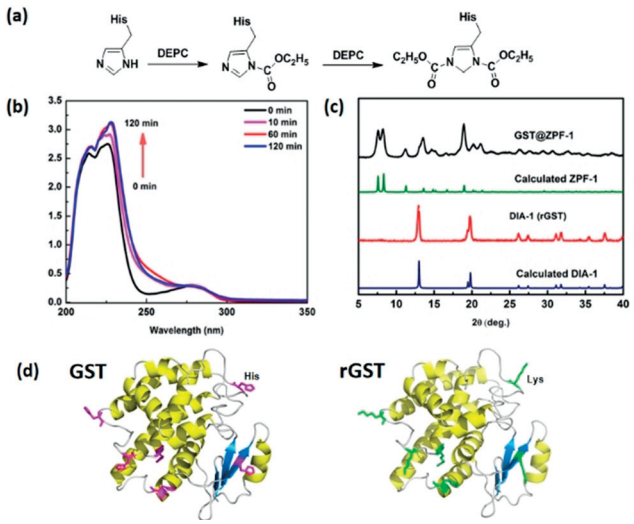

Figure 3. a) Reaction pathway of histidine imidazole groups with an excess of DEPC; b) UV/Vis spectra of BSA reacted with 10 mM DEPC recorded at 0, 10, 60, and 120 min; c) The PXRD patterns of products after adding GST or rGST; d) Modeled 3D structure of GST and rGST. His residues are shown in magenta. These His residues were mutated to Lys, shown in green.

Information, Figure S15), indicating the need for histidine during the formation of **ZPF-1**. Furthermore, we expressed glutathione S-transferase (GST), a protein with histidine, and recombinant GST (rGST), a histidine-free protein, in *Escherichia coli* to directly investigate the structure-directed role of histidine in proteins (Figure 3d). The purified GST and rGST were found to be approximately 99% pure as indicated by dodecyl sulfate, sodium salt (SDS)-Polyacrylamide gel electrophoresis (SDS-PAGE, Supporting Information, Figure S16). As predicted, GST produced the desired **sod** structure of **ZPF-1**, while rGST formed the structure of **DIA-1** (Figure 3c and Supporting Information, Table S1). Besides, we found that the addition of histidine as a co-template in the preparation of **protein@ZPF-1** can significantly increase the encapsulation efficiency of proteins in **ZPF-1** (for example, BSA encapsulation increased up to 31% in **BSA@ZPF-1**, Supporting Information, Table S2). These results revealed that histidine indeed plays a crucial role in the templating process of **ZPF-1**.

The successful incorporation of proteins into **ZPF-1** offers potential for applications, such as biocatalysis and biopharmaceutical formulation. CAT, a well-known biocatalyst, was selected as a representative enzyme to evaluate the performance of the **protein@ZPF-1** platform. The catalytic activity of **CAT@ZPF-1** was evaluated by tracking the change of H_2O_2 in solution over time (apparent rate constant, K_{obs}, Supporting Information, Figure S17). The results revealed that **CAT@ZPF-1** possesses a high activity ($K_{obs} = 3.54 \times 10^{-3}\ s^{-1}$, Supporting Information, Figure S18). The confinement of enzymes in MOFs is expected to provide protection against stress. We exposed **CAT@ZPF-1** and free CAT to heat (70 °C), organic solvent (methanol and DMF), and trypsin (an endopeptidase that cuts off the carboxyl side of the lysine and arginine residues in the polypeptide chain). As shown in

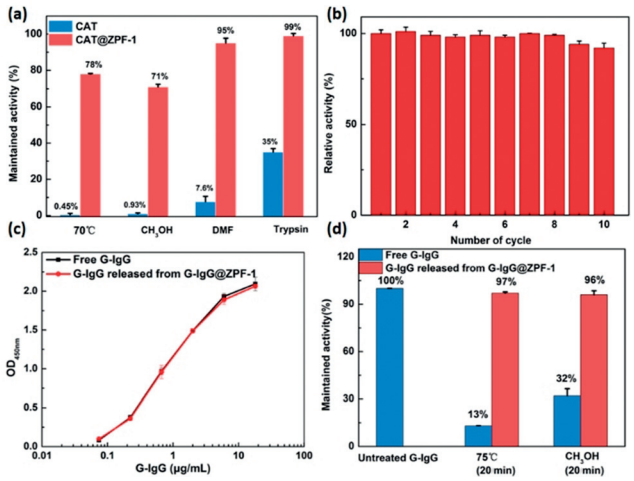

Figure 4. a) Activity of CAT and **CAT@ZPF-1** after various treatments; b) Recycling experiments of the degradation of H_2O_2 in the presence of **CAT@ZPF-1**; c) Indirect ELISA assay results of free G-IgG and G-IgG released from **G-IgG@ZPF-1**; d) Relative activity (compared with the original activity of free G-IgG) of G-IgG released from **G-IgG@ZPF-1** after various treatments.

Figure 4a, **ZPF-1**-protected CAT retained more than 70% of its original activity under all tested conditions, while free CAT demonstrated a sharp decrease (65–99%) in enzyme activity under the same conditions (Figure 4a). It is notable that **CAT@ZPF-1** can nearly retain its full activity after the treatment with DMF and trypsin. Encouraged by the good stability of **CAT@ZPF-1**, we investigated recyclability, a critical performance metric for practical applications. It was found that the enzymatic activity of **CAT@ZPF-1** exhibited no significant decrease after ten cycles (Figure 4b). **CAT@ZPF-1** exhibited no leaching and retained its crystallinity after recycling catalytic experiments (Supporting Information, Figures S19 and S20).

As important biopharmaceuticals, antibodies are a fast-growing category of therapeutic proteins that often suffer from inferior biophysical stability.[33] G-IgG antibody was selected to probe the potential of the **ZPF-1** system to protect antibodies and serve as a new biopharmaceutical formulation platform. An enzyme-linked immunosorbent assay (ELISA) was used to determine antibody activity. Our results revealed that G-IgG can be successfully encapsulated by **ZPF-1** with high efficiency ($0.32\ g\,g^{-1}$), with the encapsulation process presenting no influence on antibody activity (Figure 4c). Furthermore, as verified by a Bradford assay, the encapsulated G-IgG can be completely released from **ZPF-1** within 15 min. **G-IgG@ZPF-1** and free G-IgG were exposed at 75 °C or to methanol to test the protection effect of **ZPF-1**. The results indicate that the unprotected G-IgG lost most of its activity (more than 70%) after treatment (Figure 4d). In contrast, G-IgG encapsulated by **ZPF-1** exhibited 97% of its original activity after release from the MOF. These results highlight **ZPF-1**'s protective capabilities towards biomacromolecules, enabling it to serve as a versatile platform for biopharmaceutical formulation and storage.

In conclusion, we herein demonstrate the use of proteins as structure-directed agents in order to tune the formation of ZMOFs to afford **protein@ZPF-1**, a material that can act as a versatile in situ platform for protein encapsulation. To investigate the template mechanism, we first screened all 20 natural amino acids, which revealed that histidine played a critical role during the formation of the **sod** network. We thus modified the amount of directly added histidine or the histidine content of proteins to exert control over the MOF product and produce a pure **sod** topology ZMOF with sufficient histidine. Conversely, less histidine resulted in a **dia** + **sod** mixture or pure **dia** product. We also directly compared the histidine-free rGST protein with histidine-containing GST protein, and found histidine indeed played a key role to control the formed MOF structure. Furthermore, adding histidine as a co-template during the preparation of **protein@ZPF-1** significantly improved protein encapsulation efficiency. Moreover, as we demonstrated by control studies, the incorporation of proteins into **ZPF-1** endowed **protein@ZPF-1** with properties suitable for utility in biocatalysis or biopharmaceutical formulation. It should be noted that proteins did not exhibit a templating effect in all previously reported protein@MOF systems, such as **ZIF-8** and **ZIF-90**, since these MOFs can be obtained without adding proteins in the identical conditions. This study opens a new avenue to prepare new ZMOFs that cannot be accessed by traditional approaches, and creates a versatile strategy for the highly efficient fabrication of protein-immobilization matrixes for various advanced applications.

Acknowledgements

The authors acknowledge financial support from National Natural Science Foundation of China (21871153 and 31800793) and Tianjin Natural Science Foundation of China (18JCZDJC37300).

Conflict of interest

The authors declare no conflict of interest.

Keywords: enzyme immobilization · metal–organic frameworks · protein structure · self-assembly · template synthesis · zeolite analogues

How to cite: *Angew. Chem. Int. Ed.* **2020**, *59*, 6263–6267
Angew. Chem. **2020**, *132*, 6322–6326

[1] S.-T. Zheng, T. Wu, C. Chou, A. Fuhr, P. Feng, X. Bu, *J. Am. Chem. Soc.* **2012**, *134*, 4517–4520.
[2] M. Eddaoudi, D. F. Sava, J. F. Eubank, K. Adil, V. Guillerm, *Chem. Soc. Rev.* **2015**, *44*, 228–249.
[3] Y. Tan, F. Wang, J. Zhang, *Chem. Soc. Rev.* **2018**, *47*, 2130–2144.
[4] B. Wang, A. P. Côté, H. Furukawa, M. O'Keeffe, O. M. Yaghi, *Nature* **2008**, *453*, 207–211.
[5] H.-C. Zhou, S. Kitagawa, *Chem. Soc. Rev.* **2014**, *43*, 5415–5418.
[6] D. F. Sava, V. Ch. Kravtsov, J. Eckert, J. F. Eubank, F. Noua, M. Eddaoudi, *J. Am. Chem. Soc.* **2009**, *131*, 10394–10396.
[7] R. Babarao, J. Jiang, *J. Am. Chem. Soc.* **2009**, *131*, 11417–11425.
[8] J. Zhuang, C.-H. Kuo, L.-Y. Chou, D.-Y. Liu, E. Weerapana, C.-K. Tsung, *ACS Nano* **2014**, *8*, 2812–2819.

[9] D. Masih, V. Chernikova, O. Shekhah, M. Eddaoudi, O. F. Mohammed, *ACS Appl. Mater. Interfaces* **2018**, *10*, 11399 – 11405.
[10] F. Lyu, Y. Zhang, R. N. Zare, J. Ge, Z. Liu, *Nano Lett.* **2014**, *14*, 5761 – 5765.
[11] K. Liang, R. Ricco, C. M. Doherty, M. J. Styles, S. Bell, N. Kirby, S. Mudie, D. Haylock, A. J. Hill, C. J. Doonan, P. Falcro, *Nat. Commun.* **2015**, *6*, 7240.
[12] G. Chen, S. Huang, X. Kou, S. Wei, S. Huang, S. Jiang, J. Shen, F. Zhu, G. Ouyang, *Angew. Chem. Int. Ed.* **2019**, *58*, 1463 – 1467; *Angew. Chem.* **2019**, *131*, 1477 – 1481.
[13] F. K. Shieh, S. C. Wang, C. I. Yen, C. C. Wu, S. Dutta, L. Y. Chou, J. V. Morabito, P. Hu, M. H. Hsu, K. C. W. Wu, C. K. Tsung, *J. Am. Chem. Soc.* **2015**, *137*, 4276 – 4279.
[14] M. B. Majewski, A. J. Howarth, P. Li, M. R. Wasielewski, J. T. Hupp, O. K. Farha, *CrystEngComm* **2017**, *19*, 4082.
[15] S. Liang, X.-T. Wu, J. Xiong, M.-H. Zong, W.-Y. Lou, *Coord. Chem. Rev.* **2020**, *406*, 213149.
[16] X. Lian, Y. Fang, E. Joseph, Q. Wang, J. Li, S. Banerjee, C. Lollar, X. Wang, H.-C. Zhou, *Chem. Soc. Rev.* **2017**, *46*, 3386 – 3401.
[17] M. M. J. Treacy, S. Rao, I. Rivin, *Proceedings of the Ninth International Zeolite Conference*, Butterworth-Heinemann, Oxford, **1993**, pp. 381 – 388.
[18] D. J. Earl, M. W. Deem, *Ind. Eng. Chem. Res.* **2006**, *45*, 5449 – 5454.
[19] Q. Shi, W.-J. Xu, R.-K. Huang, W.-X. Zhang, Y. Li, P. Wang, F.-N. Shi, L. Li, J. Li, J. Dong, *J. Am. Chem. Soc.* **2016**, *138*, 16232 – 16235.
[20] Y.-H. Han, Y.-C. Liu, X.-S. Xing, C.-B. Tian, P. Lin, S.-W. Du, *Chem. Commun.* **2015**, *51*, 14481 – 14484.
[21] X. Yang, T. Liang, J. Sun, M. J. Zaworotko, Y. Chen, P. Cheng, Z. Zhang, *ACS Catal.* **2019**, *9*, 7486 – 7493.
[22] D.-M. Chen, N.-N. Zhang, C.-S. Liu, M. Du, *J. Mater. Chem. C* **2017**, *5*, 2311 – 2317.
[23] Z. Yin, Q.-X. Wang, M.-H. Zeng, *J. Am. Chem. Soc.* **2012**, *134*, 4857 – 4863.
[24] J. R. Ramirez, H. Yang, C. M. Kane, A. N. Ley, K. T. Holman, *J. Am. Chem. Soc.* **2016**, *138*, 12017—12020.
[25] C. L. Whittington, L. Wojtas, R. W. Larsen, *Inorg. Chem.* **2014**, *53*, 160 – 166.
[26] H. R. Culver, N. A. Peppas, *Chem. Mater.* **2017**, *29*, 5753 – 5761.
[27] P. Li, Q. Chen, T. C. Wang, N. A. Vermeulen, B. L. Mehdi, A. Dohnalkova, N. D. Browning, D. Shen, R. Anderson, D. A. Gómez-Gualdrón, F. M. Cetin, J. Jagiello, A. M. Asiri, J. F. Stoddart, O. K. Farha, *Chem* **2018**, *4*, 1022 – 1034.
[28] X. Lian, A. Erazo-Oliveras, J.-P. Pellois, H.-C. Zhou, *Nat. Commun.* **2017**, *8*, 2075.
[29] T. Guo, Q. Deng, G. Fang, D. Gu, Y. Yang, S. Wang, *Biosens. Bioelectron.* **2016**, *79*, 341 – 346.
[30] O. M. Yaghi, *ACS Cent. Sci.* **2019**, *5*, 1295 – 1300.
[31] X. Gu, K. Zhou, Y. Feng, J. Yao, *Chem. Lett.* **2015**, *44*, 1080 – 1082.
[32] J. Zhao, H. Li, Y. Han, R. Li, X. Ding, X. Feng, B. Wang, *J. Mater. Chem. A* **2015**, *3*, 12145 – 12148.
[33] Y. T. Adem, K. A. Schwarz, E. Duenas, T. W. Patapoff, W. J. Galush, O. Esue, *Chem. Eur. J.* **2014**, *25*, 656 – 664.

Manuscript received: January 7, 2020
Accepted manuscript online: February 3, 2020
Version of record online: March 2, 2020

